

# **Nikon Biolmaging Lab**

Let us do the imaging for you.



The Nikon Biolmaging Lab is a state-of-the-art facility located in Cambridge, Massachusetts, that provides advanced technologies to support the burgeoning regenerative medicine and biotech sector.

For more information, visit www.microscope.healthcare.nikon.com/bioimaging-lab









## EMBRYONIC STEM CELLS/INDUCED PLURIPOTENT STEM CELLS

# FGF2 Specifies hESC-Derived Definitive Endoderm into Foregut/Midgut Cell Lineages in a Concentration-Dependent Manner

Jacqueline Ameri, Anders Stählberg, Jesper Pedersen, Jenny K. Johansson, Martina M. Johannesson, Isabella Artner, Henrik Semb

Stem Cell Center, Department of Laboratory Medicine, Lund University, Lund, Sweden

**Key Words.** Human embryonic stem cells • Differentiation • Definitive endoderm • Pancreatic endoderm • FGF signaling • Fibroblast growth factor 2

#### ABSTRACT

Fibroblast growth factor (FGF) signaling controls axis formation during endoderm development. Studies in lower vertebrates have demonstrated that FGF2 primarily patterns the ventral foregut endoderm into liver and lung, whereas FGF4 exhibits broad anterior-posterior and leftright patterning activities. Furthermore, an inductive role of FGF2 during dorsal pancreas formation has been shown. However, whether FGF2 plays a similar role during human endoderm development remains unknown. Here, we show that FGF2 specifies hESC-derived definitive endoderm (DE) into different foregut lineages in a dosage-dependent manner. Specifically, increasing concentrations of FGF2 inhibits hepatocyte differentiation, whereas intermediate concentration of FGF2 promotes differentiation toward a pancreatic cell fate. At high FGF2 levels specification of midgut endoderm into small intestinal progenitors is increased at the expense of PDX1+ pancreatic progenitors. High FGF2 concentrations also promote differentiation toward an anterior foregut pulmonary cell fate. Finally, by dissecting the FGF receptor intracellular pathway that regulates pancreas specification, we demonstrate for the first time to the best of our knowledge that induction of PDX1+ pancreatic progenitors relies on FGF2-mediated activation of the MAPK signaling pathway. Altogether, these observations suggest a broader gut endodermal patterning activity of FGF2 that corresponds to what has previously been advocated for FGF4, implying a functional switch from FGF4 to FGF2 during evolution. Thus, our results provide new knowledge of how cell fate specification of human DE is controlledfacts that will be of great value for future regenerative cell therapies. STEM CELLS 2010;28:45-56

Disclosure of potential conflicts of interest is found at the end of this article.

### Introduction

Many internal organs, such as the pancreas, lung, thyroid, liver, esophagus, and stomach, are induced along the anteriorposterior axis of the definitive endoderm (DE)-derived primitive gut [1, 2]. The first sign of regionalization of the DE is the expression of specific transcription factors that are expressed in a precise manner along the anterior and posterior axis (A-P axis) of the DE, which eventually forms the primitive gut tube. In the anterior portion of the foregut endoderm, regions that are destined to become lung and thyroid express NKX2-1, whereas liver and the ventral pancreas develop from a region expressing HHEX1 and PDX1, respectively. The dorsal pancreas and duodenum originate from the posterior portion of the foregut endoderm expressing PDX1. The posterior portion of the gut endoderm that expresses CDX1 and CDX2 develops into mid- and hindgut, which later give rise to the small and large intestine [3]. FOXA1 and FOXA2 are both expressed in the entire gut tube and are thus important

for the development of all gastrointestinal tract-derived organs [4].

Fibroblast growth factor (FGF) signaling has been implicated in patterning of the gut tube along the A-P axis [3, 5, 6] and in pancreatic differentiation [7-9]. FGF4 acts as a posteriorizing growth factor with broad anterior-posterior and left-right patterning activities [3, 10, 11], whereas FGF2 plays a more restricted role [3, 12]. However, mouse studies have shown that FGF2, which is secreted from the cardiac mesoderm, patterns the adjacent multipotent ventral foregut endoderm in a concentration-dependent manner into liver and lung [12, 13]. In the absence of cardiac mesoderm and FGFs a ventral pancreatic fate is promoted [12, 14]. In contrast, an inductive role of FGF2 during dorsal pancreas formation has been demonstrated in mouse and chick [15, 16]. However, whether FGF2 plays a similar role during human endoderm organ formation has not been determined. In contrast to the chick and mouse studies, we recently demonstrated that FGF4 neither patterns hESC-derived DE nor induces PDX1+ pancreatic progenitors from hESC-derived DE [17], suggesting

Author contributions: J.A.: conception and design, collection and assembly of data, data analysis and interpretation, manuscript writing; A.S.: contribution of analysis tools (primers), data analysis and interpretation; J.P. and J.K.J.: collection of data, data interpretation; M.M.J.: contribution of analysis tools (primers), data interpretation; I.A.: data interpretation, manuscript writing; H.S.: conception and design, data interpretation, manuscript writing, financial support, administrative support, final approval of manuscript.

Correspondence: Henrik Semb, Ph.D., Lund University, Department of Laboratory Medicine, Stem Cell Center, BMC, B10, SE-221-84 Lund, Sweden. Telephone: +46 46 222 31 59; Fax: +46 46 222 36 00; e-mail: henrik.semb@med.lu.se Received August 27, 2009; accepted for publication October 20, 2009; first published online in STEM CELLS Express November 3, 2009. © AlphaMed Press 1066-5099/2009/\$30.00/0 doi: 10.1002/stem.249

STEM CELLS 2010:28:45–56 www.StemCells.com

that FGF4 is not responsible for anterior-posterior patterning of the primitive gut during human development.

The aim of the present study was to investigate whether FGF2's role in foregut endoderm specification is evolutionary conserved between mouse and human, and whether FGF2 in addition plays a more general role in primitive gut endoderm anterior-posterior patterning. Here, we show for the first time to the best of our knowledge that FGF2 specifies hESCderived DE into foregut/midgut organ-specific lineages, such as hepatic, pancreatic, pulmonary, and intestinal progenitors, in a concentration-dependent manner. Thus, FGF2's function in foregut endoderm patterning is conserved in humans. However, the posteriorizing activity of high concentrations of FGF2 on foregut-midgut specification suggests that FGF4's role in lower vertebrates may have been replaced by FGF2 during evolution. Finally, we demonstrate for the first time to the best of our knowledge that induction of PDX1<sup>+</sup> pancreatic progenitors relies on FGF2-mediated activation of the mitogen-activated protein kinase (MAPK) signaling pathway.

### MATERIALS AND METHODS

### In Vitro Culture of Human ES Cells

Undifferentiated hESCs (trypsin adapted SA181 and SA121 [Cellartis, Gothenburg, Sweden, http://www.cellartis.com], HUES-3, HUES-4, and HUES-15 obtained from D.A. Melton, Howard Hughes Medical Institute [Harvard University, Cambridge, MA]) were propagated as previously described [18, 19] protocols are also available at http://mcb.harvard.edu/melton/hues. Briefly, cells were maintained on mitotically inactivated mouse embryonic fibroblasts (Department of Experimental Biomedicine/TCF from Sahlgrenska Academy at the University of Gothenburg, Gothenburg, Sweden) in a medium containing knockout-Dulbecco's modified Eagle's medium (KO-DMEM), 10% knockout serum replacement (KO-SR), 10 ng/ml bFGF, 1% nonessential amino acids (NEAA), 1% Glutamax, 1% penicillin-streptomycin (PEST), and  $\beta$ -mercaptoethanol (all reagents from Gibco, Invitrogen, Grand Island, NY, http://www.invitrogen.com) and 10% plasmanate (Talecris Biotherapeutics Inc., Research Triangle Park, NC, http:// www.talecris.com). Cells were passaged with 0.05% trypsin/EDTA (Gibco, Invitrogen) and re-plated at a split ratio between 1:3 and

#### **Differentiation of hESCs**

hESCs were seeded at a density of 12,000-24,000 cells per cm<sup>2</sup> and cultured until confluency. hESCs were then differentiated into definitive endoderm as previously described [20]. At day 3, cells were washed with phosphate-buffered saline (PBS) and human FGF2 (Invitrogen, Carlsbad, CA, http://www.invitrogen. com) was added at different concentrations (0-256 ng/ml according to specifications in the Results) in a KO-DMEM-based medium containing 1% PEST, 1% GlutaMAX, 1% NEAA, 0.1 mM  $\beta$ -mercaptoethanol, and 12% KO-SR. Medium was changed every day. Control cultures without FGF2 were grown in parallel and cell morphology was monitored daily. Bright-field images of cells were taken on an inverted microscope (Eclipse TE2000-U) (Nikon Instruments Inc., Melville, NY, http://www.nikoninstruments.com). At each time point, two to four biological replicates were taken for each independent experiment. More specifically, each well was divided into four to five equal pieces depending on the number of time points analyzed. With the exception of the data presented in Figure S4, all of the data were generated using the HUES-3 cell line.

### **FGF Inhibition Assays**

FGF receptor inhibition assays were performed by adding SU5402 (10  $\mu$ M; Calbiochem, San Diego, http://www.emdbiosciences.com),

LY294002 (12.5  $\mu$ M; Cell Signaling Technology, Beverly, MA, http://www.cellsignal.com), and U1026 (10  $\mu$ M; Cell Signaling Technology) to the medium following DE induction at day 3. Control cultures were treated with an equal volume of the diluent dimethyl sulfoxide. Fresh medium supplemented with appropriate inhibitor was added daily. Two to three samples were taken from separate wells at different time points (days 9-12) for mRNA analysis for each independent experiment.

# RNA Extraction, Reverse Transcription, and Real-Time Polymerase Chain Reaction

Total RNA was extracted with GenElute Mammalian total RNA kit (Sigma-Aldrich, St. Louis, http://www.sigmaaldrich.com) and RNA concentrations were measured with the NanoDrop ND-1000 spectrophotometer (NanoDrop Technologies, Wilmington, DE, http://www.nanodrop.com). Reverse transcription was performed with SuperScript III, according to the manufacturer's instructions, using 2.5  $\mu M$  random hexamer and 2.5  $\mu M$  oligo(dT) (Invitrogen). Each experiment used a fixed amount of mRNA (500 ng to 1  $\mu$ g) for cDNA synthesis. Real-time polymerase chain reaction (PCR) measurements were performed on an ABI PRISM 7900HT Sequence Detector System (Applied BioSystems, Foster City, CA, http://www.appliedbiosystems.com). Twenty-microliter reactions containing 10 µl of SuperMix-UDG w/ROX, 400 nM of each primer, 0.125× SYBR Green I (all reagents from Invitrogen) were used. Primer sequences are available in supporting information Table S1. Formation of expected PCR products was confirmed by agarose gel electrophoresis and melting curve analysis. Gene expression data were normalized against ACTB or RPL7 expression. As an extra normalization control, data were also normalized against total RNA concentrations, which resulted in similar data. Real-time PCR data analysis was performed as described [21, 22]. Raw data from real-time PCR measurements were exported from SDS 2.2.1 and analyzed by Microsoft Excel graph pad. In cases where no gene expression was measured, as for some genes of untreated control cells, for example, PDX1, cycles of threshold (Ct) values were set to 45, that is, the maximum amount of cycles run. The data are shown as mean expression ± standard error of the mean (SEM). The graphs represent the fold increase in comparison to the control samples at days 9 or 11. The control sample was arbitrarily set to a value of 1.

#### Immunofluorescence Analysis of hESCs

hESCs were fixed in 4% paraformaldehyde for 15 minutes at room temperature and washed three times in PBS-T (0.1% Triton X-100 in PBS). Fixed cells were permeabilized with 0.5% Triton X-100 in PBS for 15 minutes and blocked in PBS-T supplemented with 5% normal donkey serum (Jackson Immunoresearch Laboratories, West Grove, PA, http://www.jacksonimmuno.com) for 1 hour at room temperature before overnight incubation (at 4°C) with the following primary antibodies: goat anti-FOXA-2 (Palle Serup; 1:200; Santa Cruz Biotechnology Inc., Santa Cruz, CA, http://www.scbt.com), guinea pig anti-PDX1 (Chris Wright; 1:1500; Beta Cell Biology Consortium, http://www.betacell.org), goat anti-PDX1 (Chris Wright; 1:1500; Beta Cell Biology Consortium), rabbit anti-NKX6.1 (1:4000; Beta Cell Biology Consortium), mouse anti-CDX-2 (Jonathan Draper; 1:500; BioGenex Laboratories, Inc., San Ramon, CA, http://www.biogenex.com), rabbbit anti-SOX-9 (1:500; Chemicon, Temecula, CA, http:// www.chemicon.com), rabbit anti-HNF-6 (1:400; Santa Cruz Biotechnology), mouse anti-PH-3 (1:50; Cell Signaling Technology), rabbit anti-MKi67 (1:200; Novocastra Ltd., Newcastle upon Tyne, U.K., http://www.novocastra.co.uk), rabbit anti-SOX2 (Palle Serup; 1:250; Chemicon), goat anti-albumin (1:300; Bethyl Laboratories, Montgomery, TX, http://www.bethyl.com), mouse anti-AFP (1:500; Sigma), and rabbit anti-SOX17 (1:200; Beta Cell Biology Consortium). After overnight incubation cells were washed three times for 5 minutes in PBS and incubated with corresponding fluorescent secondary antibodies (Alexa 488 and 647, and Cy3; 1:500; Jackson Immunoresearch Laboratories and

Invitrogen) for 60 minutes in PBS-T supplemented with 5% serum at room temperature. Cell nuclei were visualized by 4'-6'diamidino-2-phenylindole (DAPI) (Sigma-Aldrich; 1:1000) incubation for 4 minutes. Immunofluorescence stainings were detected and analyzed on a Zeiss Axioplan 2.

#### **Data Analysis**

The percentage of ALB+ cells was calculated using Imaris Imaging software (Bitplane, Zurich, Switzerland, http://www.bitplane.com). Ten randomly selected fileds were chosen for each parameter. The total area of nuclei was estimated by DAPI staining, whereas the ALB+ area was visualized by ALB antibody staining. Finally, the percentage of  $ALB^+$  cells was calculated by dividing the  $ALB^+$  area by the  $DAPI^+$  area. Imaging software was also used in a similar manner for quantification of PDX1, CDX2, SOX17, and PDX1<sup>+</sup>/NKX6-1<sup>+</sup> cells. The percentage of PDX1<sup>+</sup>/NKX6-1<sup>+</sup> nuclei was calculated by dividing the NKX6-1+ area by the PDX1+ area. This could be performed as all NKX6-1<sup>+</sup> cells colocalize with PDX1. For quantification of PDX1/SOX9, PDX1/HNF6, PDX1/CDX2, and PDX1/PH3 double-positive cells, the analysis tool in Adobe Photoshop CS3 Extended version 10.0.1 was used. Roughly, 1000-2000 PDX1+ cells from two to four separate experiments were counted in total for each double staining. All data were statistically analyzed by multivariate comparison (one-way ANOVA) with Bonferroni correction. All values are depicted as mean ± SEM and considered significant if p < .05.

#### RESULTS

# Activin A/Wnt3a-Treated hESCs Spontaneously Differentiate into Foregut and Midgut Endoderm

Human ESCs were differentiated into DE by Activin A/ Wnt3a treatment in low serum for 3 days as previously described [20]. Formation of anterior DE was confirmed by an upregulation of SOX17 [23], CXCR4 [24], CER1 [25], GSC [26], HHEX [27], and FOXA2 [4, 28] (supporting information Figs. S1, S2A). Furthermore, the self-renewal gene OCT-4, which is highly upregulated in the undifferentiated hESCs, was downregulated both at day 3 and at day 11 (supporting information Figs. S1, S12). In addition, SOX17 and FOXA2 co-staining of hESC-derived DE at day 3 showed that more than 90% of the cells treated with Activin A/Wnt3a co-express SOX17 and FOXA2 (supporting information Fig. S2B). By assessing the expression of characteristic foregut/ midgut markers, we show that a fraction of the FOXA2<sup>+</sup>/ AFP+ hESCs treated with Activin A/Wnt3a differentiate into foregut endoderm, including liver progenitors (Fig. 1C, 1D, supporting information Figs. S3, S4), and midgut endoderm (Fig. 5). Altogether, these findings suggest that anterior foregut endoderm differentiates into liver but not into other foregut-derived cell types, such as pancreatic and pulmonary endoderm in the absence of exogenous FGF2.

### Low Doses of FGF2 Promote a Hepatic Cell Fate, Whereas Intermediate FGF2 Levels Induce a Pancreatic Cell Fate

To test whether FGF2 is capable of directing differentiation of foregut endoderm into a pancreatic fate (presumably a dorsal pancreatic fate), the ability of different FGF2 concentrations (0, 4, 16, 32, 64, and 256 ng/ml) to induce *PDX1* expression was assessed. The concentrations were in part based on mouse explant studies [12, 29]. The differentiation protocol (Fig. 1A) was applied on five different cell lines, HUES-3—subclone 52, HUES-4, HUES-15, and the trypsin-adapted SA181 and SA121—to allow more generally applicable conclusions. Cells

grew denser and in larger clusters when treated with higher FGF2 concentrations (16-256 ng/ml) (Fig. 1B). Hepatocyte-like cells were primarily seen in hESC cultures treated with no FGF2 or low doses of FGF2 (4 ng/ml) (Fig. 1B, 1C). Increasing FGF2 concentrations downregulated expression of the cardiac marker *TNNT2* and the hepatic markers albumin (*ALB*) [30], *ONECUT1* (previously known as *HNF6*) [31, 32], and *HNF4A* [33], whereas *HHEX* [34] expression was only moderately reduced. The latter is probably due to the fact that *HHEX* is also expressed in anterior foregut-derived organs, such as in lung progenitor cells, which are induced at this high FGF2 concentration (see below) (Fig. 1D, supporting information Fig. S3).

Albumin expression was also confirmed at the protein level. Although abundant ALB<sup>+</sup> cells were seen in the absence (10.4%) of and at 4 ng/ml FGF2 (7.3%), no ALB<sup>+</sup> cells were observed at 256 ng/ml (Fig. 1C). Furthermore, all the cells in the samples treated with Activin A/Wnt3a and 4 ng/ml FGF2 expressed  $\alpha$ -fetoprotein (AFP) at day 11 (Fig. 1C; inset, supporting information Fig. S4).

To determine pancreatic cell fate commitment, a combination of markers associated with pancreatic progenitors was chosen including PDX1 [35, 36], SOX9 [37, 38], NKX6-1 [39], PTF1A [40, 41], NGN3 [42, 43], and FOXA2 [44]. Expression of posterior foregut-associated markers was detected in all samples at days 9 and 11. SOX9 expression was upregulated with increasing FGF2 concentrations, whereas PDX1 and NKX6-1 expression peaked at 64 ng/ml and was reduced at 256 ng/ml (Fig. 2A). Low levels of NKX6-1 and NGN3 were (in the majority of the experiments) detected already at day 9 (supporting information Fig. S5) but expression increased at later time points (Fig. 2A). However, PTF1A expression was detected only at low mRNA levels (data not shown). FOXA2 was expressed in all samples both at day 9 (supporting information Fig. S5) and day 11 (Fig. 2A) but was not influenced by FGF2 treatment.

PDX1<sup>+</sup> cells were exclusively found in samples treated with 32-256 ng/ml FGF2 (Fig. 2B). The number of PDX1<sup>+</sup> cells was significantly higher in FGF2-treated cells (32-256 ng/ml) compared to the number of control cells (not treated with FGF2). The highest number of PDX1<sup>+</sup> cells (15%–20%) was obtained in the presence of 64 ng/ml FGF2 at day 11 (Fig. 2B). Robust induction of *PDX1* and *NKX6-1* mRNA expression at 64 ng/ml FGF2 was confirmed in multiple experiments using five different hESC lines (supporting information Fig. S6).

Although all pancreatic tissue is derived from Pdx1expressing multipotent progenitor cells [45], Pdx1<sup>+</sup> cells are also found in the posterior stomach, duodenum, and CNS (only mRNA transcript). Therefore, expression of additional pancreatic markers was used to verify differentiation toward a pancreatic cell fate. All PDX1<sup>+</sup> cells co-expressed FOXA2 (Fig. 3). Furthermore, the vast majority of the PDX1<sup>+</sup> cells co-expressed SOX9 and ONECUT1, whereas only a few PDX1<sup>+</sup>/CDX2<sup>+</sup> cells were detected (Fig. 3). PDX1 and NKX6-1 are normally co-expressed in mouse and human pancreatic epithelium but not in the duodenum and stomach [39, 46]. Notably, cells co-expressing PDX1 and NKX6-1 were found only in samples treated with 32 ng/ml (data not shown) and 64 ng/ml FGF2 (Fig. 3). The highest number of PDX1+/ NKX6-1<sup>+</sup> cells was detected at 64 ng/ml (9%). Only a fraction of the PDX1<sup>+</sup> cells co-expressed NKX6-1, whereas all NKX6-1<sup>+</sup> cells co-expressed PDX1. Interestingly, when the concentration of FGF2 was raised to 256 ng/ml, formation of pancreatic endoderm was blocked (Fig. 4). This was apparent by the appearance of fewer PDX1+ cells, but more importantly none of the remaining PDX1+ cells co-expressed NKX6-1 (Fig. 4). Thus, exogenous FGF2 promotes conversion of hESC-derived foregut endoderm into a pancreatic cell

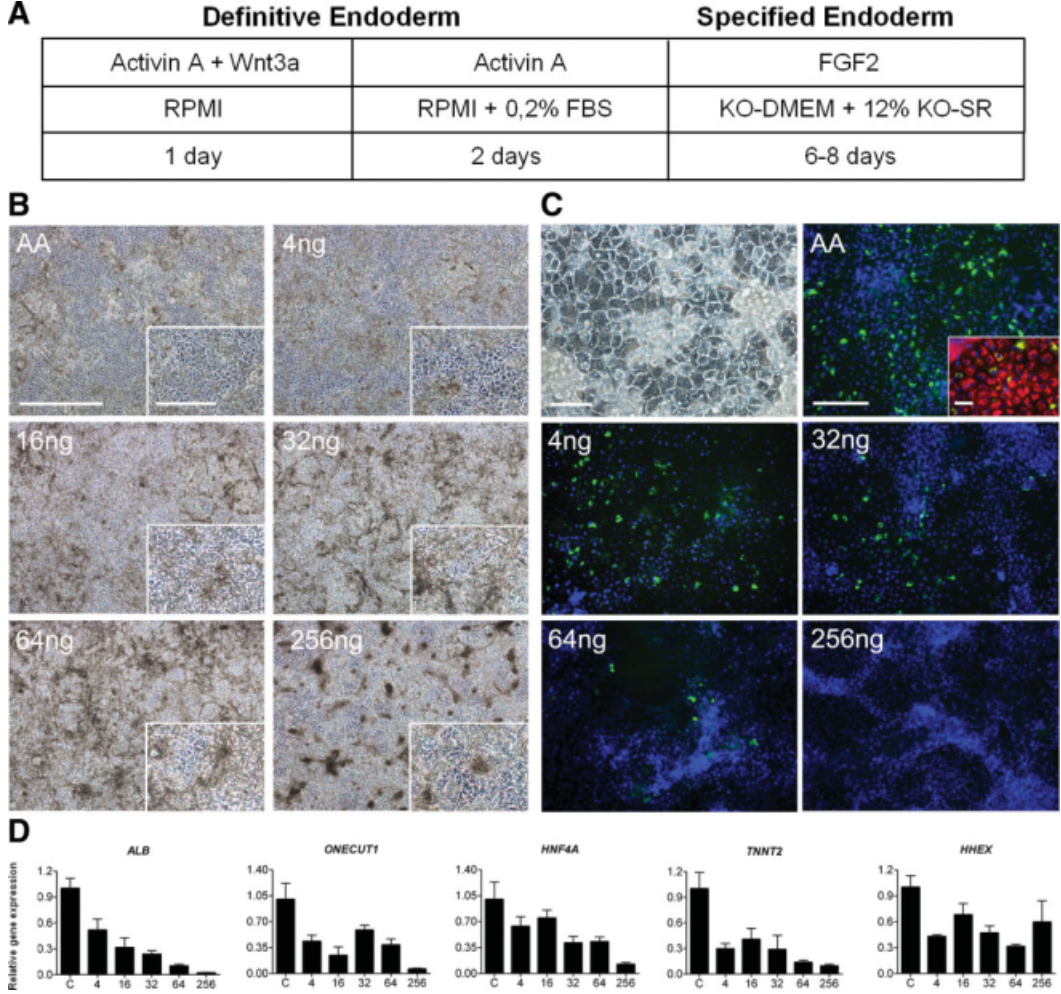


**Figure 1.** Increased concentration of FGF2 inhibits specification of hepatocyte-like cells. (**A**): A schematic representation of the two-step differentiation procedure for specification of mesendoderm/definitive endoderm (DE). The differentiation protocol includes a first step to direct differentiation of mesendoderm/DE and a second step to specify mesendoderm/DE. (**B**): Phase contrast pictures of differentiated hESCs at the end of step 2 (day 11). The highest number of hepatocyte-like cells was seen in cultures treated with only Activin A (AA) or low FGF2 concentration (4 ng/ml). Increasing FGF2 concentrations resulted in denser colonies and formation of thick clusters. Insets show higher magnification of a randomly chosen area. Scale bar = 100 μm for all the pictures except the insets that are 50 μm. (**C**): Albumin stainings of hESCs treated with different FGF2 concentrations (ng/ml). Phase contrast image shows higher magnification of hepatocyte-like cells. The number of ALB<sup>+</sup> cells decreased with increasing FGF2 concentration. In fact, at 256 ng/ml no ALB<sup>+</sup> cells were seen. The estimated number of ALB<sup>+</sup> cells at different FGF2 concentrations is as follows: AA; 10.4%, 4 ng/ml; 7.3%, 32 ng/ml; 3.3%, 64 ng/ml; 0.24%, and 256 ng/ml; 0%. Inset shows that all ALB<sup>+</sup> cells (green) co-express AFP (red). Nuclear counterstaining with DAPI is shown in blue. Scale bars: 100 μm for the phase contrast picture; 300 μm for the pictures with albumin staining; and 50 μm for the inset. (**D**): Hepatocyte associated markers *ALB*, *HNF4A*, and *ONECUT1* and the cardiac marker *TNNT2* were all down-regulated with increasing FGF2 concentrations (ng/ml) in comparison to the control sample treated only with Activin A. *HHEX* was slightly downregulated already at 4 ng/ml FGF2. Samples were taken for real-time polymerase chain reaction analysis at day 11. The data are shown as mean expression ± SEM (n = 4). The graphs represent the fold increase in comparison to that detected in the control samples at day 11. The control sample w

fate (Fig. 2A, supporting information Fig. S6), whereas it inhibits hepatic cell fate (Fig. 1C, 1D, supporting information Figs. S3, S6) in a concentration-dependent manner.

Expression of proliferation marker phospho-histone-H3 (PH3) [47] was detected only in a few PDX1<sup>+</sup> cells at day 11 (Fig. 3), suggesting that at this time point there is no general proliferation.

### High Doses of FGF2 Direct Differentiation of hESC-Derived DE into Anterior Foregut and Small Intestinal Cells

As the expression of the hepatocyte markers ALB, HNF4A, and ONECUT1 decreased with increasing FGF2 concentra-

tions (Fig. 1C, 1D), the expression level of the anterior foregut-associated marker *SOX-2* [48, 49] increased, with the highest level observed at 256 ng/ml (supporting information Fig. S7). Consistently, Sox-2 expression was confined to anterior foregut derivatives, such as esophagus, lung, and stomach in E13.5 mouse embryos (supporting information Fig. S8C).

Since lung and thyroid arise from the same region of the anterior foregut endoderm, the expression pattern of markers associated with these organs was assessed at the mRNA level (supporting information Fig. S7). The observation that the thyroid-specific marker thyroglobulin (*TG*) [50] was downregulated with increasing FGF2 concentrations (data

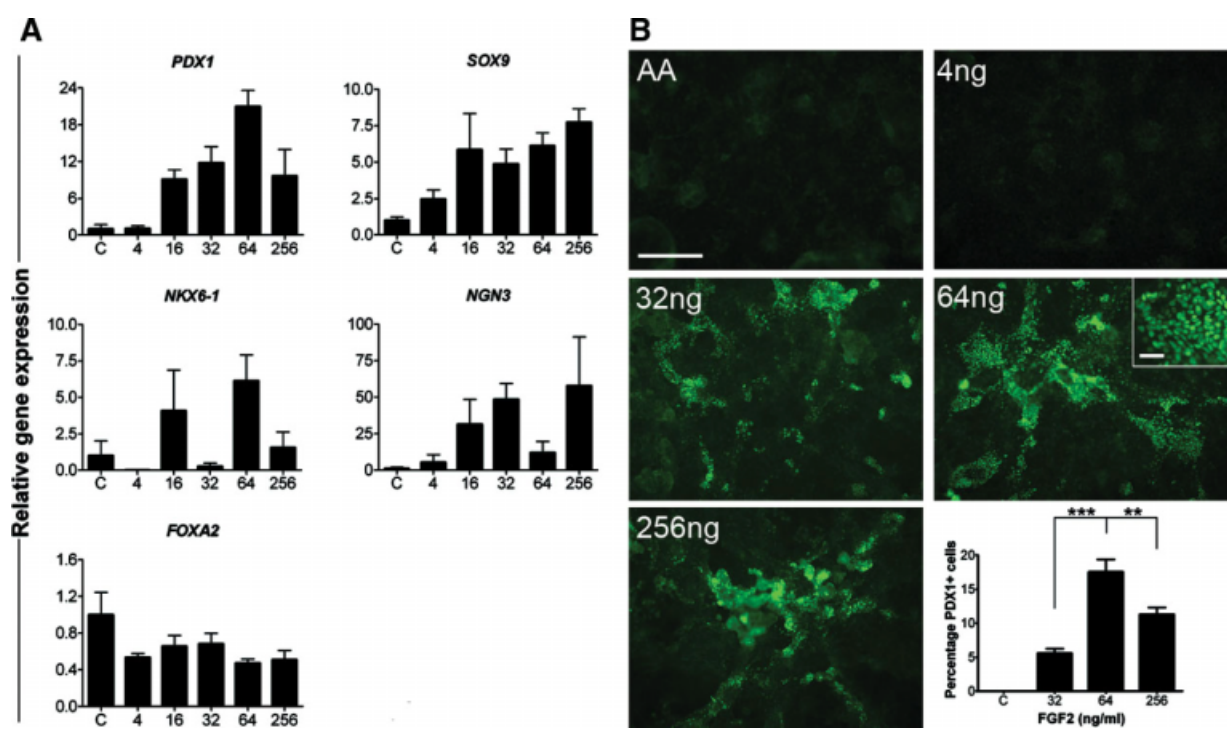


Figure 2. FGF2 induces expression of pancreas specific genes in a concentration-dependent manner. (A): PDXI and SOX9 were upregulated in all FGF2-treated samples except when treated with low FGF2 concentration (4 ng/ml). Both PDXI and NKX6-1 had peak expression at 64 ng/ml, whereas NGN3 was downregulated at this concentration. FOXA2 was detected in all samples and remained unchanged. Data are shown as mean expression  $\pm$  SEM (n=4). The graphs represent the fold increase in comparison to that detected in the control samples at day 11. The control sample was arbitrarily set to a value of 1. (B): PDX1 stainings of hESCs treated with different FGF2 concentrations. PDX1 $^+$  cells could not be observed in cultures treated with Activin A only or 4 ng/ml FGF2, whereas PDX1 $^+$  cells were always present in cultures treated with 32, 64, and 256 ng/ml FGF2. The highest percentage of PDX1 $^+$  cells was seen at 64 ng/ml. This was assessed both by microscopy and the use of the Imaris Imaging software. The data are presented as the mean + SEM (n=7-10). The following p values were attained: control versus 32 ng/ml (p<0.01), control versus 64 ng/ml (p<0.01), control versus 256 ng/ml (p<0.01), and 64 ng/ml versus 256 ng/ml (p<0.01). p<0.05 was considered to be significant. Scale bars: 300  $\mu$ m for the PDX1 staining pictures; 40  $\mu$ m for the inset. Abbreviation: FGF, fibroblast growth factor.

not shown), but that the earliest marker of lung and thyroid specification NKX2-1 [51] was upregulated at 256 ng/ml, suggested induction of pulmonary lineages. However, the pulmonary surfactant protein C (SP-C), [52], and Clara cell 10 kDa protein (CC10) [53] mRNAs were undetectable, suggesting that the NKX2-1<sup>+</sup> cells represent early lung progenitor cells. Additional markers associated with, but not restricted to, the induction of a pulmonary cell fate, including FGF10 [54], SPRY2 [55], SHH [56, 57], and the SHH receptor PTCH1 [58], were also significantly upregulated at the highest FGF2 concentration (supporting information Fig. S7). To address whether the lack of mature lung markers was due to too low FGF2 concentration, 500 ng/ml FGF2 was also tested. However, this resulted in no change in NKX2-1 expression, and no induction of SP-C or CC10 expression (data not shown). These results deviate from a recent study on mouse ES cells [13] where both 50 and 500 ng/ml of FGF2 was sufficient to induce SP-C mRNA expression. Thus, it remains to be determined if the absence of more mature lung markers is caused by the lack of additional inductive factors required during human lung development.

Expression of the midgut/hindgut markers *CDX2* [59] and *MNX1* significantly increased at the highest FGF2 concentration (256 ng/ml), suggesting that a high concentration of FGF2 also induced formation of intestinal cell types (supporting information Fig. S7). CDX2 expression was confirmed at the protein level, confirming the highest number of CDX2<sup>+</sup> cells at 256 ng/

ml (Fig. 5). Moreover, CDX2<sup>+</sup> cells co-expressed FOXA2, confirming endodermal rather than trophectodermal identity of the CDX2<sup>+</sup> cells [60] (Fig. 6A). In contrast, expression of another hindgut marker *CDX1* [61] remained unchanged (supporting information Fig. S7) and the large intestine marker CDX4 [62] was not detected at any concentration. Altogether, these findings support the notion that high levels of FGF2 also promote midgut specification. The fact that 52.3% of the CDX2<sup>+</sup> cells were positive for the MKI67 antigen [63] suggests that CDX2<sup>+</sup> cells are formed by proliferation and differentiation (supporting information Fig. S8B).

To further characterize the PDX1<sup>+</sup>/NKX6-1<sup>-</sup> cell population at 256 ng/ml, PDX1/CDX2 and PDX1/SOX2 co-localization studies were carried out. Although a few PDX1<sup>+</sup>/CDX2<sup>+</sup> cells were identified, the majority of the PDX1<sup>+</sup> cells were CDX2<sup>-</sup> (Fig. 4). Furthermore, none of the PDX1<sup>+</sup> cells coexpressed SOX2 (Fig. 4). On the basis of similar colocalization studies in E18.5 mouse embryos, we conclude that Pdx1<sup>+</sup>/Sox2<sup>+</sup> and Pdx1<sup>+</sup>/Cdx2<sup>+</sup> cells represent posterior stomach and posterior midgut (duodenal) cell types, respectively (supporting information Figs. S8A–S8C). The Pdx1<sup>+</sup>/Sox2<sup>-</sup>/Cdx2<sup>-</sup> cells may represent either anterior midgut cells or differentiated pancreatic cells.

In summary, high levels of FGF2 direct differentiation of foregut endoderm into anterior fates, such as pulmonary lineages, and increase midgut endoderm specification at the expense of pancreatic posterior foregut endoderm commitment.

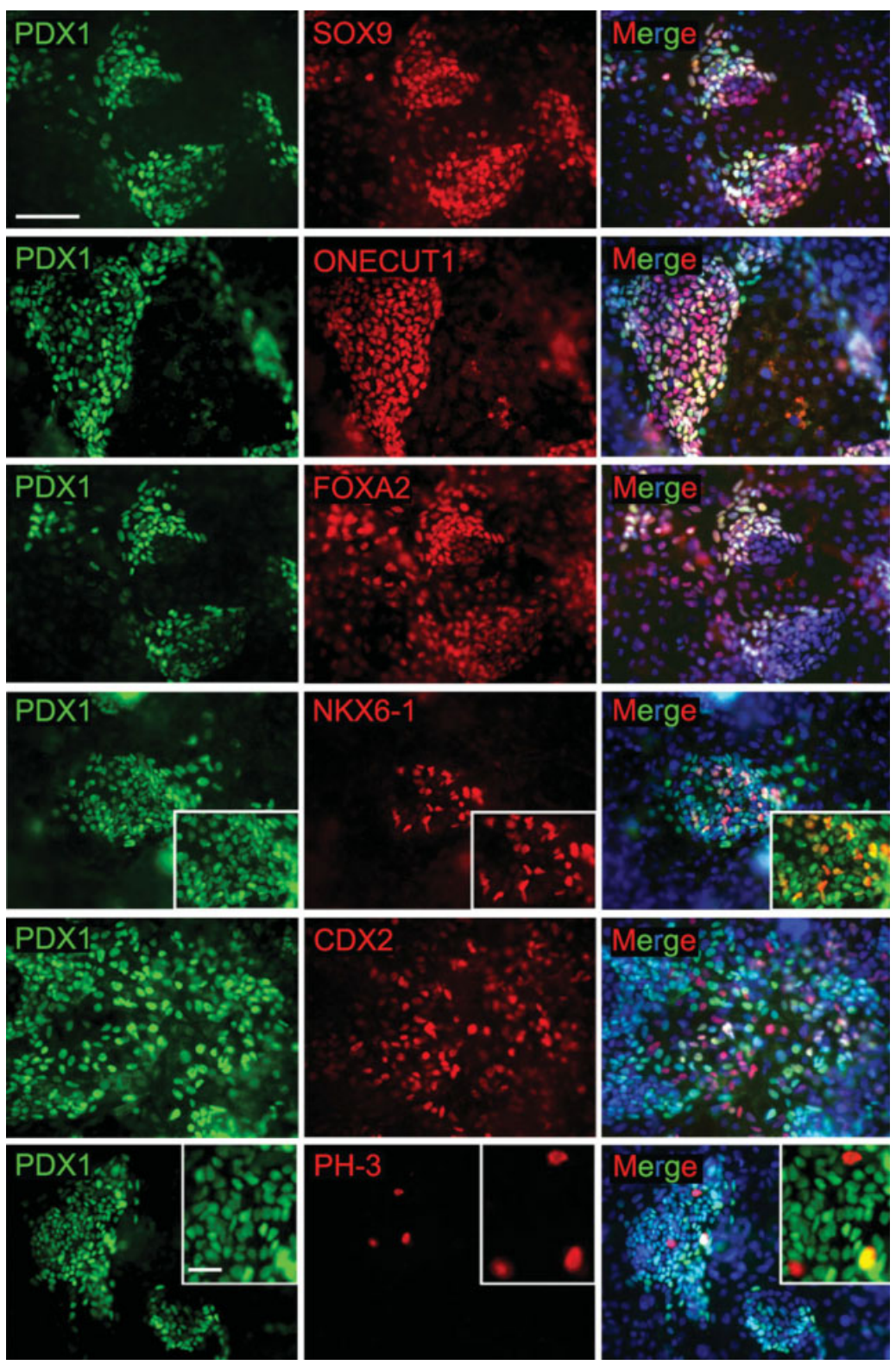


Figure 3. Sixty-four nanograms per milliliter FGF2 induces PDX1 $^+$  pancreatic endoderm. Immunofluorescence analysis of the PDX1 $^+$  cell population at 64 ng/ml FGF2. All PDX1 $^+$  cells co-expressed FOXA2 (100%). The majority of the PDX1 $^+$  cells was also SOX9 $^+$  (95%) and ONECUT1 $^+$  (95.2%). Notably, a fraction of the PDX1 $^+$  cells co-expressed NKX6-1 (9.0%). Furthermore, the majority of the PDX1 $^+$  cells were negative for the intestinal marker CDX2 (93%) and the proliferation marker PH-3 (99.6%). Scale bars: 150 μm for all of the staining pictures except for the insets, which are 50 μm for the PDX1/NKX6-1 and 40 μm for the PDX1/PH3.

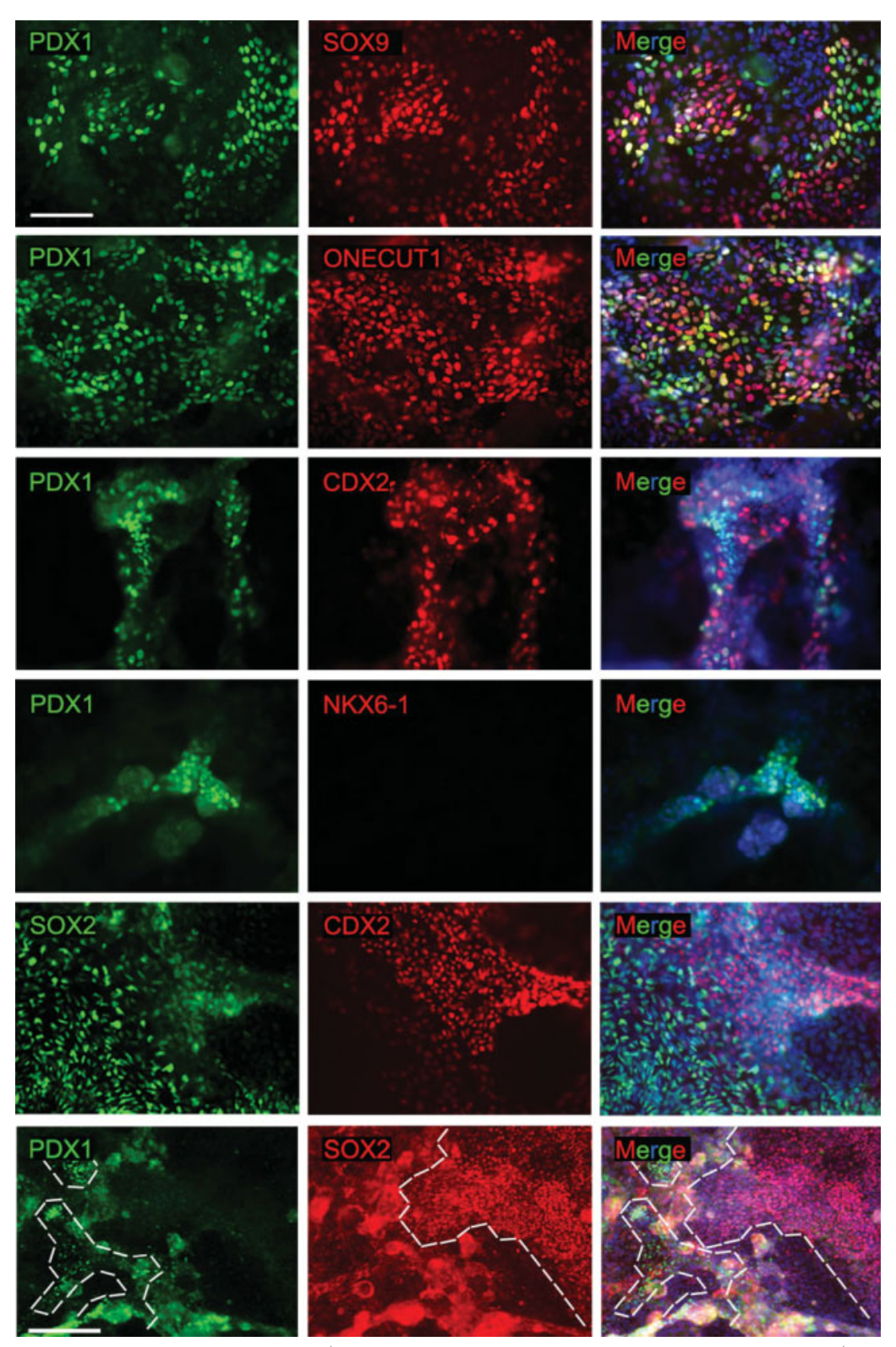


Figure 4. Immunofluorescence analysis of the PDX1 $^+$  cell population at 256 ng/ml FGF2. The majority of the PDX1 $^+$  cells were SOX9 (87.4%) and ONECUT1 positive (95.4%). Although a few PDX1 $^+$ /CDX2 $^+$  cells (7.1%) were found, the majority of PDX1 $^+$  cells (92.9%) were CDX2 negative. Importantly, none of the PDX1 $^+$  cells co-expressed NKX6-1 or SOX2. In addition, all SOX2 $^+$  cells were CDX2 negative. Scale bars = 150 μm for all pictures except for the PDX1/SOX2 staining, that is, 300 μm.

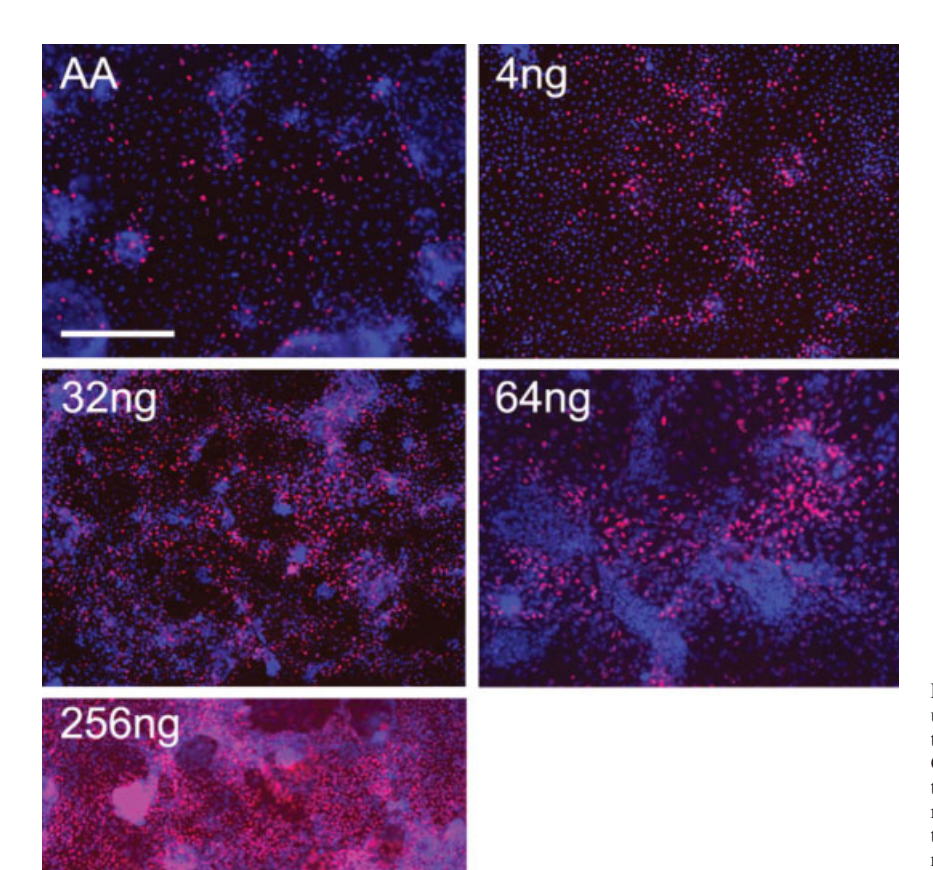


Figure 5. The number of CDX2<sup>+</sup> cells is upregulated with increasing FGF2 concentration. Immunofluorescence analysis of the CDX2<sup>+</sup> cell population demonstrated that the number of CDX2<sup>+</sup> cells (red) was upregulated with increasing FGF2 concentrations, except at 64 ng/ml. The highest number was observed at 256 ng/ml. The estimated number of CDX2<sup>+</sup> cells at different FGF2 concentrations is as follows: AA; 26.9%, 4 ng/ml; 20.1%, 32 ng/ml; 37.8%, 64 ng/ml; 25.6%, and 256 ng/ml; 44.7%. Nuclear counterstaining with DAPI is shown in blue. Scale bar: 300  $\mu$ m.

# ERK1/2 Mitogen-Activated Protein Kinase Signaling Is Required for PDX1 Induction

Multiple FGFs (FGF1, FGF2, FGF4, FGF7, and FGF10) and their receptors (FGFR1 and FGFR2) are expressed and involved in early development of the pancreas [64–66]. Monitoring expression of FGF2, FGF4, FGF7, and FGF10 during hESC differentiation confirmed that all ligands are expressed (supporting information Fig. S9). Upregulation of FGF10 mRNA levels at 256 ng/ml FGF2 may be explained by expression in pulmonary and potentially also esophagus progenitors induced at this concentration (see above).

There are at least four different tyrosine kinase receptors (FGFR1–FGFR4) that bind different FGF ligands with varying affinities. In addition, alternative splicing of FGFR1–FGFR3 generates "IIIb" and "IIIc" isoforms, which display distinct expression patterns and ligand specificities [67]. FGF2 acts mainly via the IIIc isoforms of FGFR1, FGFR2, and FGFR3, but it also binds with lower affinity to FGFR1b and FGFR4 [67, 68]. By binding to their respective receptors (FGFRs), FGFs activate several signal transduction pathways, including phosphatidylinositol-3 kinase (PI3K) and ERK1/2 mitogen-activated protein kinases (MAPKs). FGFR mRNA expression analysis demonstrated that FGFR1–FGFR4 were detected in all samples (Fig. 7A, supporting information Fig. S10). Furthermore, a tendency toward elevated levels of FGFR1 and FGFR3 and decreased

levels of *FGFR2* and *FGFR4* was seen with increasing FGF2 concentrations (Fig. 7A, supporting information Fig. S10).

To determine whether FGFR-mediated signaling is required for the induction of PDX1 transcription, the effect of the FGFR tyrosine kinase inhibitor SU5402, MAPK inhibitor, U1026, and PI3K inhibitor, LY294002, was investigated (Fig. 7B). Treatment with SU5402 significantly decreased the number of PDX1<sup>+</sup> cells, indicating that FGF2 (64 ng/ml) mediates induction of PDXI<sup>+</sup> cells via FGFR signaling. In addition, treatment with FGF2 in the presence of U1026 diminished PDX1 expression, indicating that activation of the MAPK pathway is necessary for induction of PDX1. In contrast, when cells were treated with FGF2 in the presence of LY294002, PDX1 expression remained unchanged, suggesting that an active PI3K pathway is not required for induction of PDX1 (Fig. 7C, supporting information Fig. S11). In summary, these results demonstrate that the MAPK pathway, and not the PI3K pathway, is necessary for FGF2-mediated induction of PDX1 expression.

## DISCUSSION

FGF2 secreted from the cardiac mesoderm is a powerful inducer of foregut-derived cell lineages, including hepatic, and pulmonary cell types [12, 14], whereas notochord secreted

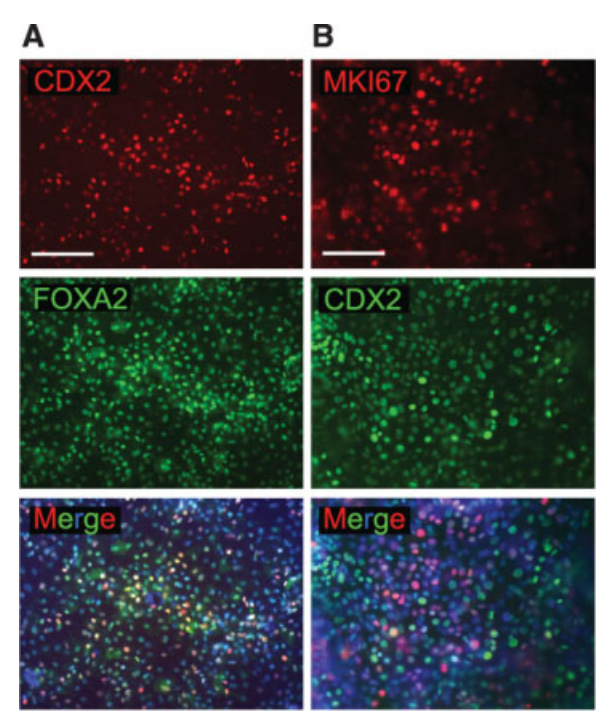


**Figure 6.** CDX2 $^+$  cells represent endodermal cells. (A): Co-localization studies of CDX2 and FOXA2 demonstrated that all CDX2 $^+$  cells (red) co-express the endodermal marker FOXA2 (green). Scale bar: 150  $\mu$ m. (B): 52.3% of the CDX2 $^+$  cells (green) co-expressed MKI67 (red) at 256 ng/ml. Scale bar: 150  $\mu$ m.

FGF2 controls dorsal pancreas induction [15, 16]. Importantly, it is the ability of multipotent foregut endodermal progenitors to sense the timing and concentration of FGF2 that determines the outcome of their fate determination. Currently, there is a tremendous interest in generating foregut endodermderived functional cell types, such as pancreatic beta cells and hepatocytes, from human pluripotent stem cells to be used in regenerative medicine, toxicology, and drug discovery. Governed by the developmental biological principles that normally control foregut endoderm specification, numerous multistage/multifactor protocols for directing mature foregutderived cells from hESCs have been reported [20, 69-73]. However, to establish less complex and more robust protocols, there is a need to further understand the mechanism of action of individual growth and differentiation factors in specification of human pluripotent stem cells toward foregutderived cell lineages. Thus, the objective of this study is not to recapitulate the effects of FGF during pancreatic endocrine progression, but to expand the knowledge of how FGF signaling, in particular, FGF2, controls foregut endoderm specification. Here, we show that FGF2 specifies hESC-derived DE into foregut/midgut organ-specific lineages, such as hepatic, pancreatic, pulmonary, and intestinal progenitors, in a concentration-dependent manner. Notably, in contrast to previous studies in chick and mouse [3, 10], where it was demonstrated that FGF4 exhibits significantly higher anterior-posterior gut patterning activity than FGF2, at least at low concentrations (1-10 ng/ml), our results suggest that FGF2, but not FGF4, exhibits gut tube patterning activities in the hESC system. Instead, FGF4's main role is to promote cell viability [17]. Altogether, these results suggest that FGF4's role in foregutmidgut patterning may have been replaced by FGF2 during evolution. Additionally, this discrepancy may be explained by the fact that previous studies in mouse and chick only examined the effects of low FGF2 concentrations (1-10 ng/ml) [10, 74, 75]. The reproducibility of responses in several hESC lines suggests detection of a core response, relevant to human organ/tissue development. Finally, we demonstrate for the first time to the best of our knowledge that induction of PDX1<sup>+</sup> pancreatic progenitors relies on FGF2-mediated activation of the MAPK signaling pathway.

### Definitive Endoderm—Naïve or Pre-specified?

Signaling pathways controlling DE development are conserved between invertebrates and mammalians, including primates [76]. Thus, mesendoderm/DE can be reliably generated from both mouse and human ESCs through addition of Activin A [20, 77-81]. However, it remains unclear whether the hESC-derived DE represents a naïve or a prepatterned endoderm. In our study, a fraction of the SOX17<sup>+</sup>/FOXA2<sup>+</sup> hESCs treated with Activin A only differentiate toward foregut and midgut/hindgut endoderm characterized by FOXA2<sup>+</sup>/ AFP<sup>+</sup>/ALB<sup>+</sup> and FOXA2/AFP<sup>+</sup>/CDX2<sup>+</sup> expression, respectively. Thus, hESC-induced DE most likely represents a heterogeneous cell population, consisting of distinct foregut and midgut/hindgut progenitors. We propose that these progenitors respond differently to specific FGF2 concentrations. Specifically, within the foregut endoderm progenitors, induction of hepatic fate occurs by default (most likely via endogenous FGF2) and is sustained at low FGF2 concentrations (4 ng/ml), whereas intermediate and higher FGF2 concentrations (32-256 ng/ml) inhibit hepatic cell formation and instead promote pancreatic and pulmonary cell fates.

# Intermediate Levels of FGF2 Induce PDX1<sup>+</sup> Pancreatic Endoderm

Ventral pancreatic cell fate occurs by default in mouse anterior ventral foregut endoderm [14], whereas intermediate FGF2 concentrations promote dorsal pancreas induction [15]. The observations that *PDX1* expression is lost when *FGFR* signaling is inhibited and that induction of PDX1<sup>+</sup>/NKX6-1<sup>+</sup> pancreatic endoderm requires intermediate levels of exogenous FGF2 suggest that the hESC-derived pancreatic progenitors represent dorsal pancreatic endoderm. However, it cannot be excluded that formation of human ventral pancreatic endoderm, in contrast to mouse/chicken ventral pancreatic endoderm, requires FGF2 signaling.

# FGF2 Induces Pancreatic Endoderm Via the MAPK Signaling Pathway

We show that FGFR1-FGFR4 are expressed during hESC differentiation, indicating that exogenous FGF2 acts via any of these receptors. To dissect by which intracellular signaling pathway FGF2 induces pancreatic endoderm, various inhibitors of FGF signaling were used. Inhibition of FGFR and MAPK signaling diminished PDX1 expression, whereas a block of the PI3K pathway did not affect induction of pancreatic endoderm. Previous studies have demonstrated that the MAPK pathway stimulates the expansion of murine pancreatic epithelial cells downstream of FGF7 and FGF10 [82]. However, the MAPK pathway has not been implicated in the induction of the  $PDXI^+$  pancreatic progenitor cells to date. Thus, these results support a novel model for FGF2-mediated induction of PDX1 expression and pancreatic endoderm formation via MAPK signaling. It remains to be investigated if the mechanism by which FGF2 induces pancreatic endoderm in the hESCs also applies to other FGF ligands such as FGF7 and FGF10. Interestingly, in a recent study by Melton and colleagues [51], PKC signaling was implicated in the

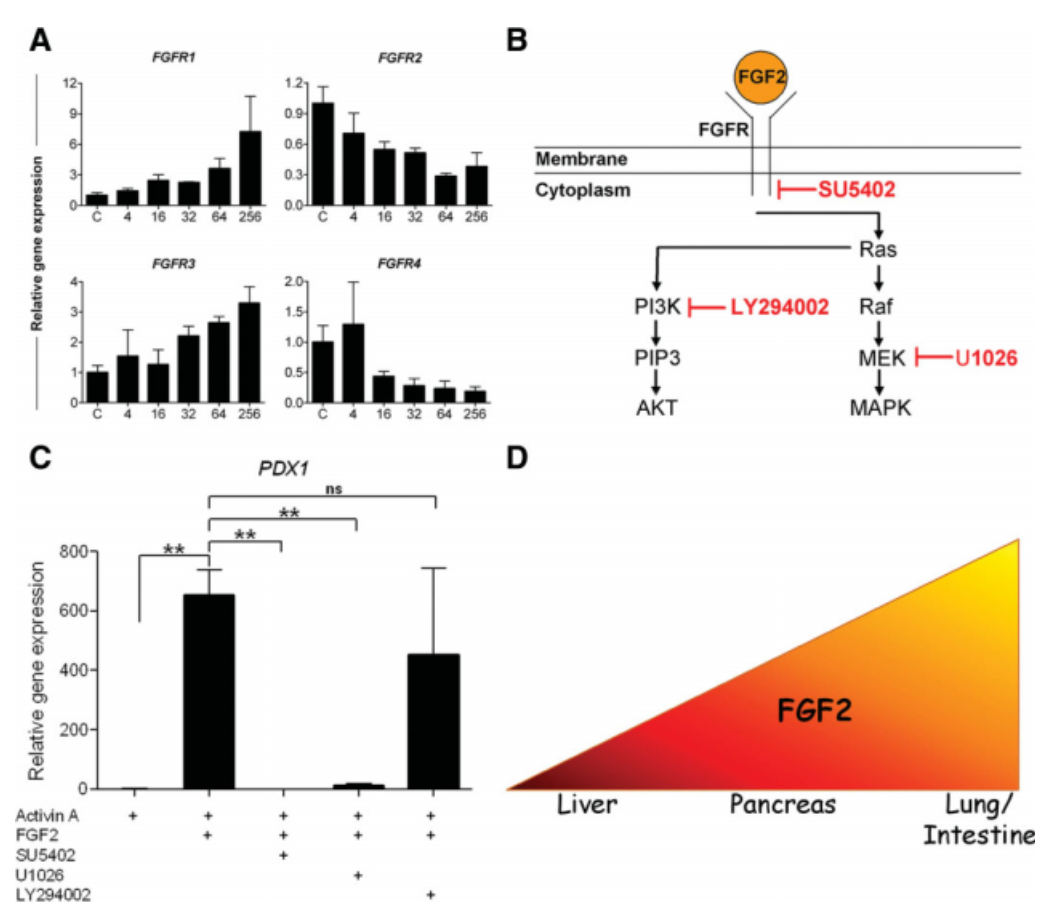


Figure 7. PDXI induction by FGF2 is mediated by MAPK signaling. (A): FGF receptor mRNA expression at day 11. FGFR1 and FGFR3 expression were upregulated with higher FGF2 concentrations, whereas FGFR2 and FGFR4 were downregulated. (B): Schematic view of the intracellular signaling pathways activated by FGF2, and the activity of pharmacological inhibitor. (C): Inhibition of FGF signaling diminished PDXI expression in vitro. Antagonizing FGF signaling (64 ng/ml) with SU5402 (10  $\mu$ M) or the MAPK inhibitor, U1026 (10  $\mu$ M), significantly reduced PDXI expression, whereas treatment with the P13K inhibitor, LY294002 (12.5  $\mu$ M), had no effect on PDXI expression. (D): Schematic illustration of how different FGF2 concentrations induce specification of hESC-derived DE into liver, pancreas, and lungs. Low FGF2 concentrations promote differentiation toward hepatocyte-like cells (marked by ALB expression) and moderate FGF2 levels differentiate the hESC-derived foregut endoderm into pancreas (marked by PDXI expression), whereas high concentrations promote differentiation toward pulmonary and intestinal cells (marked by NKX2-I and CDX2 expression). All samples for real-time polymerase chain reaction analysis were taken at day 11. Data are shown as mean expression  $\pm$  SEM, n = 3-4 for FGFR expression and n = 4-6 for inhibition analysis. The graphs represent the fold increase in comparison to that detected in the control samples at day 11. As PDXI expression could not be detected in the majority of the control samples, the Ct values in these samples were set to 45, which correspond to the total number of cycles. The control sample was arbitrarily set to a value of 1. Abbreviaton: FGF, fibroblast growth factor; FGFR, FGF receptor.

induction and maintenance of  $PDXI^+$  cells. Thus, it will be interesting to investigate the interaction between PKC-MAPK signaling during pancreas development both in mouse and in humans.

### **CONCLUSIONS**

In summary, these findings provide new insight into how FGF signaling regulates human endoderm development and may be of value when designing new hESCs-based differentiation protocols for future regenerative cell therapies.

#### ACKNOWLEDGMENTS

The work was supported by the Juvenile Diabetes Research Foundation (JDRF), Swedish Research Council, Swedish Diabe-

tes Association Research Foundation, Stem Cell Center, Lund University, and JDRF-Center for Beta Cell Therapy in Europe (supported by JDRF and EU). I.A. is the recipient of a JDRF career development award and supported by the Swedish Research Council. We thank Cellartis AB and Dr. Douglas Melton for supplying hESC lines and Drs. Serup and Wright for supply of reagents. We also thank Karolina Landerman, Ann-Katrin Häger, and Ingar Nilsson for technical assistance. A.S. is currently affiliated with Lundberg Laboratory for Cancer, Department of Pathology, Sahlgrenska Academy at the University of Gothenburg, Gothenburg, Sweden.

# DISCLOSURE OF POTENTIAL CONFLICTS OF INTEREST

The authors indicate no potential conflicts of interest.

#### REFERENCES

- 1 Grapin-Botton A, Melton DA. Endoderm development: From patterning to organogenesis. Trends Genet 2000;16(3):124–130.
- 2 Wells JM, Melton DA. Vertebrate endoderm development. Annu Rev Cell Dev Biol 1999;15:393–410.
- 3 Dessimoz J, Opoka R, Kordich JJ et al. FGF signaling is necessary for establishing gut tube domains along the anterior-posterior axis in vivo. Mech Dev 2006;123(1):42–55.
- 4 Ang SL, Wierda A, Wong D et al. The formation and maintenance of the definitive endoderm lineage in the mouse: Involvement of HNF3/ forkhead proteins. Development 1993;119(4):1301–1315.
- 5 Cardoso WV, Lu J. Regulation of early lung morphogenesis: Questions, facts and controversies. Development 2006;133(9):1611–1624.
- 6 Rossi JM, Dunn NR, Hogan BL et al. Distinct mesodermal signals, including BMPs from the septum transversum mesenchyme, are required in combination for hepatogenesis from the endoderm. Genes Dev 2001;15(15):1998–2009.
- 7 Bhushan A, Itoh N, Kato S et al. Fgf10 is essential for maintaining the proliferative capacity of epithelial progenitor cells during early pancreatic organogenesis. Development 2001;128(24):5109–5117.
- 8 Dichmann DS, Miller CP, Jensen J et al. Expression and misexpression of members of the FGF and TGFbeta families of growth factors in the developing mouse pancreas. Dev Dyn 2003;226(4):663–674.
- 9 Hart A, Papadopoulou S, Edlund H. Fgf10 maintains notch activation, stimulates proliferation, and blocks differentiation of pancreatic epithelial cells. Dev Dyn 2003;228(2):185–193.
- 10 Wells JM, Melton DA. Early mouse endoderm is patterned by soluble factors from adjacent germ layers. Development 2000;127(8):1563–1572.
- 11 Yamauchi H, Miyakawa N, Miyake A et al. Fgf4 is required for leftright patterning of visceral organs in zebrafish. Dev Biol 2009;332(1): 177–185.
- 12 Serls AE, Doherty S, Parvatiyar P et al. Different thresholds of fibroblast growth factors pattern the ventral foregut into liver and lung. Development 2005;132(1):35–47.
- 13 Roszell BR, Mondrinos MJ, Seaton A et al. Efficient derivation of alveolar type II cells from embryonic stem cells for in vivo application. Tissue Eng Part A 2009;15(11):3351–3365.
- 14 Deutsch G et al. A bipotential precursor population for pancreas and liver within the embryonic endoderm. Development 2001;128(6): 871–881.
- 15 Hebrok M, Kim SK, Melton DA. Notochord repression of endodermal Sonic hedgehog permits pancreas development. Genes Dev 1998; 12(11):1705–1713.
- 16 Kim SK, MacDonald RJ. Signaling and transcriptional control of pancreatic organogenesis. Curr Opin Genet Dev 2002;12(5):540–547.
- 17 Johannesson M, Ståhlberg A, Åmeri J et al. FGF4 and retinoic acid direct differentiation of hESCs into PDX1-expressing foregut endoderm in a time- and concentration-dependent manner. PLoS One 2009;4(3):e4794.
- 18 Cowan CA et al. Derivation of embryonic stem-cell lines from human blastocysts. N Engl J Med 2004;350(13):1353–1356.
- 19 Heins N, Englund MC, Sjöblom C et al. Derivation, characterization, and differentiation of human embryonic stem cells. Stem Cells 2004; 22(3):367–376.
- 20 D'Amour KA, Bang AG, Eliazer S et al. Production of pancreatic hormone-expressing endocrine cells from human embryonic stem cells. Nat Biotechnol 2006;24(11):1392–1401.
- 21 Bustin SA. Absolute quantification of mRNA using real-time reverse transcription polymerase chain reaction assays. J Mol Endocrinol 2000;25(2):169–193.
- 22 Stahlberg A, Aman P, Ridell B et al. Quantitative real-time PCR method for detection of B-lymphocyte monoclonality by comparison of kappa and lambda immunoglobulin light chain expression. Clin Chem 2003;49(1):51–59.
- 23 Kanai-Azuma M, Kanai Y, Gad JM et al. Depletion of definitive gut endoderm in Sox17-null mutant mice. Development 2002;129(10): 2367–2379.
- 24 McGrath KE, Koniski AD, Maltby KM et al. Embryonic expression and function of the chemokine SDF-1 and its receptor, CXCR4. Dev Biol 1999;213(2):442–456.
- 25 Bouwmeester T, Kim S, Sasai Y et al. Cerberus is a head-inducing secreted factor expressed in the anterior endoderm of Spemann's organizer. Nature 1996;382(6592):595–601.
- 26 Blum M, Gaunt SJ, Cho KW et al. Gastrulation in the mouse: The role of the homeobox gene goosecoid. Cell 1992;69(7):1097–1106.
- 27 Morrison GM, Oikonomopoulou I, Migueles RP et al. Anterior definitive endoderm from ESCs reveals a role for FGF signaling. Cell Stem Cell 2008;3(4):402–415.

- 28 Ang SL, Rossant J. HNF-3 beta is essential for node and notochord formation in mouse development. Cell 1994;78(4):561–574.
- 29 Jung J, Zheng M, Goldfarb M et al. Initiation of mammalian liver development from endoderm by fibroblast growth factors. Science 1999; 284(5422):1998–2003.
- 30 Gualdi R, Bossard P, Zheng M et al. Hepatic specification of the gut endoderm in vitro: Cell signaling and transcriptional control. Genes Dev 1996;10(13):1670–1682.
- 31 Landry C, Clotman F, Hioki T et al. HNF-6 is expressed in endoderm derivatives and nervous system of the mouse embryo and participates to the cross-regulatory network of liver-enriched transcription factors. Dev Biol 1997;192(2):247–257.
- 32 Rausa F, Samadani U, Ye H et al. The cut-homeodomain transcriptional activator HNF-6 is coexpressed with its target gene HNF-3 beta in the developing murine liver and pancreas. Dev Biol 1997;192(2):228–246.
- 33 Li J, Ning G, Duncan SA. Mammalian hepatocyte differentiation requires the transcription factor HNF-4alpha. Genes Dev 2000;14(4): 464-474.
- 34 Keng VW, Yagi H, Ikawa M et al. Homeobox gene Hex is essential for onset of mouse embryonic liver development and differentiation of the monocyte lineage. Biochem Biophys Res Commun 2000;276(3): 1155–1161.
- 35 Jonsson J, Carlsson L, Edlund T et al. Insulin-promoter-factor 1 is required for pancreas development in mice. Nature 1994;371(6498): 606–609.
- 36 Offield MF, Jetton TL, Labosky PA et al. PDX-1 is required for pancreatic outgrowth and differentiation of the rostral duodenum. Development 1996;122(3):983–995.
- 37 Seymour PA, Freude KK, Tran MN et al. SOX9 is required for maintenance of the pancreatic progenitor cell pool. Proc Natl Acad Sci U S A 2007;104(6):1865–1870.
- 38 Lynn FC, Smith SB, Wilson ME et al. Sox9 coordinates a transcriptional network in pancreatic progenitor cells. Proc Natl Acad Sci U S A 2007;104(25):10500–10505.
- 39 Pedersen JK, Nelson SB, Jorgensen MC et al. Endodermal expression of Nkx6 genes depends differentially on Pdx1. Dev Biol 2005;288(2): 487–501.
- 40 Kawaguchi Y, Cooper B, Gannon M et al. The role of the transcriptional regulator Ptf1a in converting intestinal to pancreatic progenitors. Nat Genet 2002;32(1):128–134.
- 41 Zhou Q et al. A multipotent progenitor domain guides pancreatic organogenesis. Dev Cell 2007;13(1):103–114.
- 42 Schwitzgebel VM, Law AC, Rajagopal J et al. Expression of neurogenin3 reveals an islet cell precursor population in the pancreas. Development 2000;127(16):3533–3542.
- 43 Gradwohl G et al. Neurogenin3 is required for the development of the four endocrine cell lineages of the pancreas. Proc Natl Acad Sci U S A 2000;97(4):1607–1611.
- 44 Lee CS, Sund NJ, Vatamaniuk MZ et al. Foxa2 controls Pdx1 gene expression in pancreatic beta-cells in vivo. Diabetes 2002;51(8): 2546–2551.
- 45 Gu G, Brown JR, Melton DA. Direct lineage tracing reveals the ontogeny of pancreatic cell fates during mouse embryogenesis. Mech Dev 2003:120(1):35–43
- 46 Lyttle BM, Li J, Krishnamurthy M et al. Transcription factor expression in the developing human fetal endocrine pancreas. Diabetologia 2008;51(7):1169–1180.
- 47 Goto H, Tomono Y, Ajiro K et al. Identification of a novel phosphorylation site on histone H3 coupled with mitotic chromosome condensation. J Biol Chem 1999;274(36):25543–25549.
- 48 Ishii Y, Rex M, Scotting PJ et al. Region-specific expression of chicken Sox2 in the developing gut and lung epithelium: Regulation by epithelial-mesenchymal interactions. Dev Dyn 1998;213(4):464– 475
- 49 Gontan C, de Munck A, Vermeij M et al. Sox2 is important for two crucial processes in lung development: branching morphogenesis and epithelial cell differentiation. Dev Biol 2008;317(1):296–309.
- 50 Barzon L, Boscaro M, Pacenti M et al. Evaluation of circulating thyroid-specific transcripts as markers of thyroid cancer relapse. Int J Cancer 2004;110(6):914–920.
- 51 Costa RH, Kalinichenko VV, Lim L. Transcription factors in mouse lung development and function. Am J Physiol Lung Cell Mol Physiol 2001;280(5):L823–L838.
- 52 Kelly SE, Bachurski CJ, Burhans MS et al. Transcription of the lungspecific surfactant protein C gene is mediated by thyroid transcription factor 1. J Biol Chem 1996;271(12):6881–6888.
- 53 Bolton SJ, Pinnion K, Marshall CV et al. Changes in Clara cell 10 kDa protein (CC10)-positive cell distribution in acute lung injury following repeated lipopolysaccharide challenge in the rat. Toxicol Pathol 2008;36(3):440–448.

- 54 Min H, Danilenko DM, Scully SA et al. Fgf-10 is required for both limb and lung development and exhibits striking functional similarity to Drosophila branchless. Genes Dev 1998;12(20): 3156-3161.
- 55 Mailleux AA, Tefft D, Ndiaye D et al. Evidence that SPROUTY2 functions as an inhibitor of mouse embryonic lung growth and morphogenesis. Mech Dev 2001;102(1-2):81-94.
- 56 Miller LA, Wert SE, Whitsett JA. Immunolocalization of sonic hedgehog (Shh) in developing mouse lung. J Histochem Cytochem 2001; 49(12):1593–1604.
- 57 Pepicelli CV, Lewis PM, McMahon AP. Sonic hedgehog regulates branching morphogenesis in the mammalian lung. Curr Biol 1998; 8(19):1083–1086.
- 58 Bellusci S, Furuta Y, Rush MG et al. Involvement of Sonic hedgehog (Shh) in mouse embryonic lung growth and morphogenesis. Development 1997;124(1):53–63.
- 59 Freund JN, Domon-Dell C, Kedinger M et al. The Cdx-1 and Cdx-2 homeobox genes in the intestine. Biochem Cell Biol 1998;76(6): 957–969
- 60 Tolkunova E, Cavaleri F, Eckardt S et al. The caudal-related protein cdx2 promotes trophoblast differentiation of mouse embryonic stem cells. Stem Cells 2006;24(1):139–144.
- 61 van den Akker E, Forlani S, Chawengsaksophak K et al. Cdx1 and Cdx2 have overlapping functions in anteroposterior patterning and posterior axis elongation. Development 2002;129(9):2181– 2193
- 62 Gamer LW, Wright CV. Murine Cdx-4 bears striking similarities to the Drosophila caudal gene in its homeodomain sequence and early expression pattern. Mech Dev 1993;43(1):71–81.
- 63 Scholzen T, Gerdes J. The Ki-67 protein: From the known and the unknown. J Cell Physiol 2000;182(3):311–322.
- 64 Hart AW, Baeza N, Apelqvist A et al. Attenuation of FGF signalling in mouse beta-cells leads to diabetes. Nature 2000;408(6814): 864–868.
- 65 Le Bras S, Miralles F, Basmaciogullari A et al. Fibroblast growth factor 2 promotes pancreatic epithelial cell proliferation via functional fibroblast growth factor receptors during embryonic life. Diabetes 1998;47(8):1236–1242.
- 66 Ye F, Duvillie B, Scharfmann R. Fibroblast growth factors 7 and 10 are expressed in the human embryonic pancreatic mesenchyme and promote the proliferation of embryonic pancreatic epithelial cells. Diabetologia 2005;48(2):277–281.
- 67 Ornitz DM, Xu J, Colvin JS et al. Receptor specificity of the fibroblast growth factor family. J Biol Chem 1996;271(25):15292–15297.

- 68 Ornitz DM, Itoh N. Fibroblast growth factors. Genome Biol 2001; 2(3):REVIEWS300.
- 69 Jiang J, Au M, Lu K et al. Generation of insulin-producing islet-like clusters from human embryonic stem cells. Stem Cells 2007;25(8): 1940–1953.
- 70 Kroon E, Martinson LA, Kadoya K et al. Pancreatic endoderm derived from human embryonic stem cells generates glucose-responsive insulin-secreting cells in vivo. Nat Biotechnol 2008;26(4):443–452.
- 71 Shim JH, Kim SE, Woo DH et al. Directed differentiation of human embryonic stem cells towards a pancreatic cell fate. Diabetologia 2007;50(6):1228–1238.
- 72 Hay DC, Fletcher J, Payne C et al. Highly efficient differentiation of hESCs to functional hepatic endoderm requires ActivinA and Wnt3a signaling. Proc Natl Acad Sci U S A 2008;105(34):12301–12306.
- 73 Pei H, Yang Y, Xi J et al. Lineage restriction and differentiation of human embryonic stem cells into hepatic progenitors and zone 1 hepatocytes. Tissue Eng Part C Methods 2009;15(1):95–104.
- 74 Dessimoz J, Grapin-Botton A. Pancreas development and cancer: Wnt/beta-catenin at issue. Cell Cycle 2006;5(1):7–10.
- 75 Kumar M, Jordan N, Melton D et al. Signals from lateral plate mesoderm instruct endoderm toward a pancreatic fate. Dev Biol 2003; 259(1):109–122.
- 76 Grapin-Botton A, Constam D. Evolution of the mechanisms and molecular control of endoderm formation. Mech Dev 2007;124(4): 253–278.
- 77 D'Amour KA, Agulnick AD, Eliazer S et al. Efficient differentiation of human embryonic stem cells to definitive endoderm. Nat Biotechnol 2005;23(12):1534–1541.
- 78 Gadue P, Huber TL, Paddison PJ et al. Wnt and TGF-beta signaling are required for the induction of an in vitro model of primitive streak formation using embryonic stem cells. Proc Natl Acad Sci U S A 2006;103(45):16806–16811.
- 79 Kubo A, Shinozaki K, Shannon JM et al. Development of definitive endoderm from embryonic stem cells in culture. Development 2004; 131(7):1651–1662.
- 80 Tada S et al. Characterization of mesendoderm: A diverging point of the definitive endoderm and mesoderm in embryonic stem cell differentiation culture. Development 2005;132(19):4363–4374.
- 81 Yasunaga M, Era T, Furusawa C et al. Induction and monitoring of definitive and visceral endoderm differentiation of mouse ES cells. Nat Biotechnol 2005;23(12):1542–1550.
- 82 Elghazi L, Cras-Méneur C, Czernichow P et al. Role for FGFR2IIIb-mediated signals in controlling pancreatic endocrine progenitor cell proliferation. Proc Natl Acad Sci U S A 2002;99(6):3884–3889.



See www.StemCells.com for supporting information available online.